Supporting information

High Energy Density of All Screen-Printable Solid-State Microsupercapacitor Integrated by Graphene/CNTs as Hierarchical Electrodes

Jui-Kung Chih[†], Anif Jamaluddin[#], Fuming Chen[^], Jeng-Kuei Chang[%,] and Ching-Yuan Su[†#%*]

[†] *Dep. of Mechanical Engineering, National Central University, Tao-Yuan 32001, Taiwan*

[#] *Graduate Institute of Energy Engineering, National Central University, Tao-Yuan 32001, Taiwan*

[^] *School of Physics and Telecommunication Engineering, South China Normal University, Guangzhou 510006, China*

[%] *Department of Materials Science and Engineering, National Chiao Tung University,*

Hsinchu 30010, Taiwan

To whom correspondence should be addressed: (C. Y. Su) cysu@ncu.edu.tw

Table S1. The comparison of BET surface area on ECG and CNTs/ECG.

ECG	Surface Area	0.4552 ± 0.0265 (m^2/g)
	Correlation Coefficient	0.9968877
	Langmuir Surface Area	0.5611 ± 0.0229 (m^2/g)
	Correlation Coefficient	0.9983400
CNTs/ECG	Surface Area	0.6898 ± 0.0072 (m^2/g)
	Correlation Coefficient	0.9998380
	Langmuir Surface Area	0.9808 ± 0.0208 (m^2/g)
	Correlation Coefficient	0.9995510

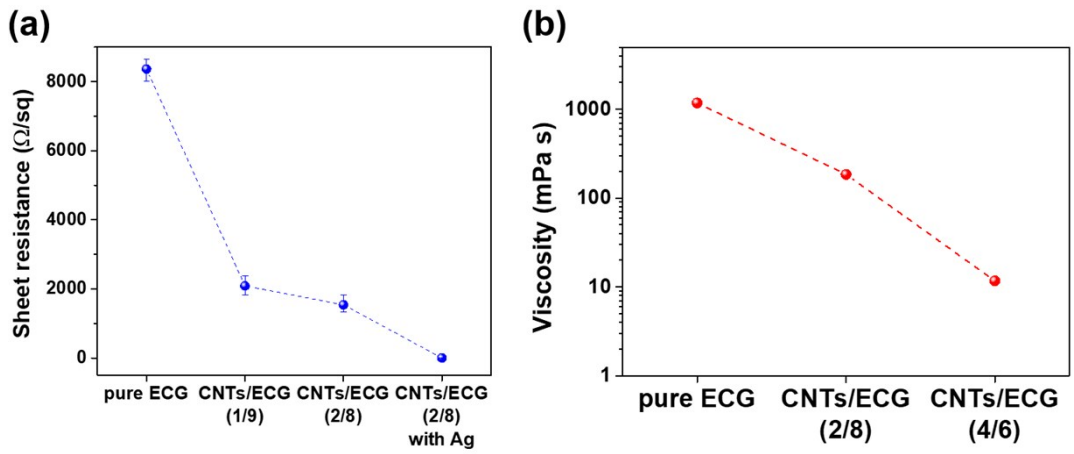

Figure S1. (a) The correlation of the sheet resistance with the various electrode conditions, and (b) the viscosity with increased the ratio of CNTs in ECG/CNTs composites.

Table S2 The parametric study on the geometric dimension of MSCs electrodes

MSC devices without Ag current collector							
Device number	1	3	5	6	7	8	9
Width(W) (mm)	4	3	2	1.5	1	0.5	0.4
Interspace(I) (mm)	0.8						
Length(L) (mm)	15.2						
Capacitance (mF/cm^2)	1.7	1.8	3.4	3.7	4.4	4.7	4.5
MSC devices with Ag current collector			
Device number	10	11	12
Width(W) (mm)	1		
Interspace(I) (mm)	0.8	1	1.2
Length(L) (mm)	15.2		
Capacitance (mF/cm^2)	12.6	12.1	10.4

* Here the two terminal electrodes (T) with the fixed at 2 mm.

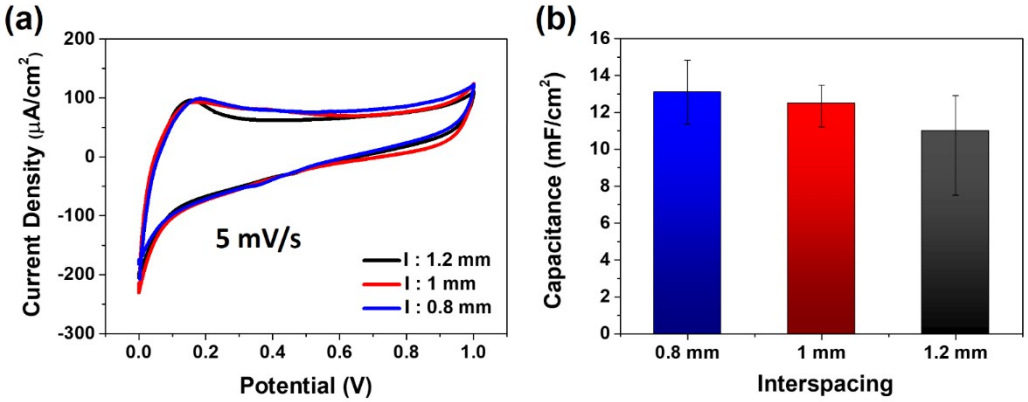

Figure S2. (a) CV curves, and (b) the capacitance comparison of the devices with the a different interspace.

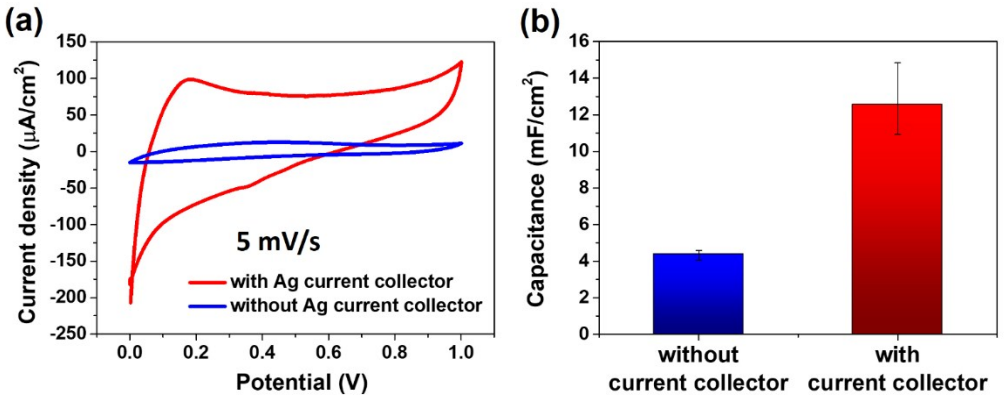

Figure S3. (a) CV curves, and (b) the capacitance comparison of the devices with and without Ag current collector.

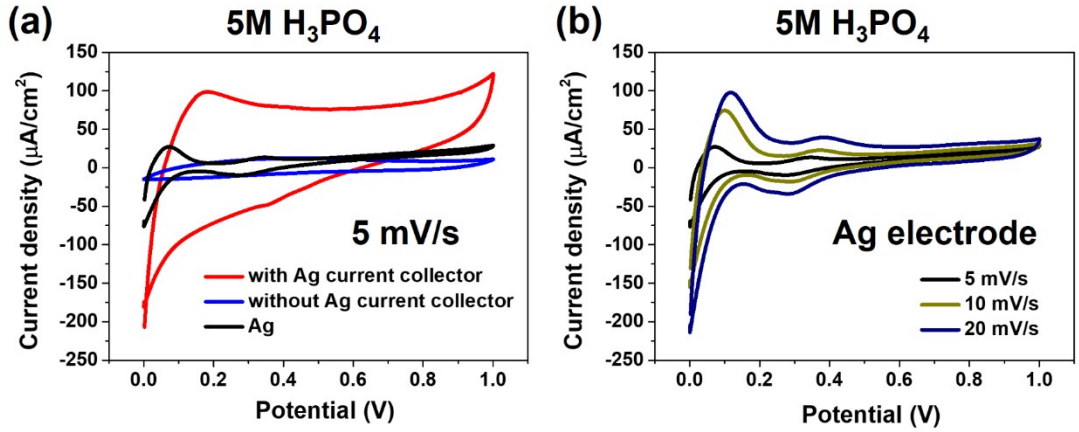

Figure S4. (a) The CV curves for devices with pristine Ag electrode and the ECG/CNTs with and without Ag as a current collector. (b) The CV curves of pristine Ag electrodes at the various scan rate.

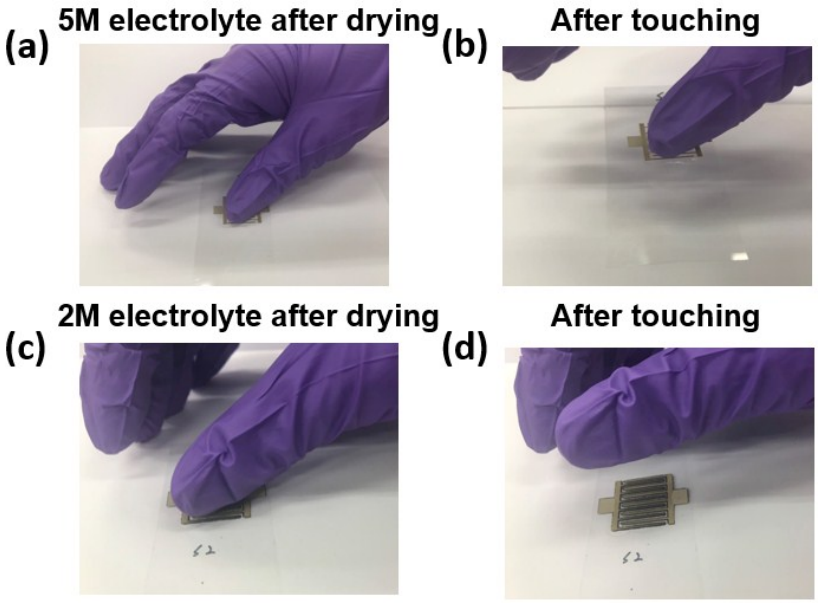

Figure S5. The adhesive testing on (a-b)the 5M electrolyte and (c-d)The 2M electrolyte.

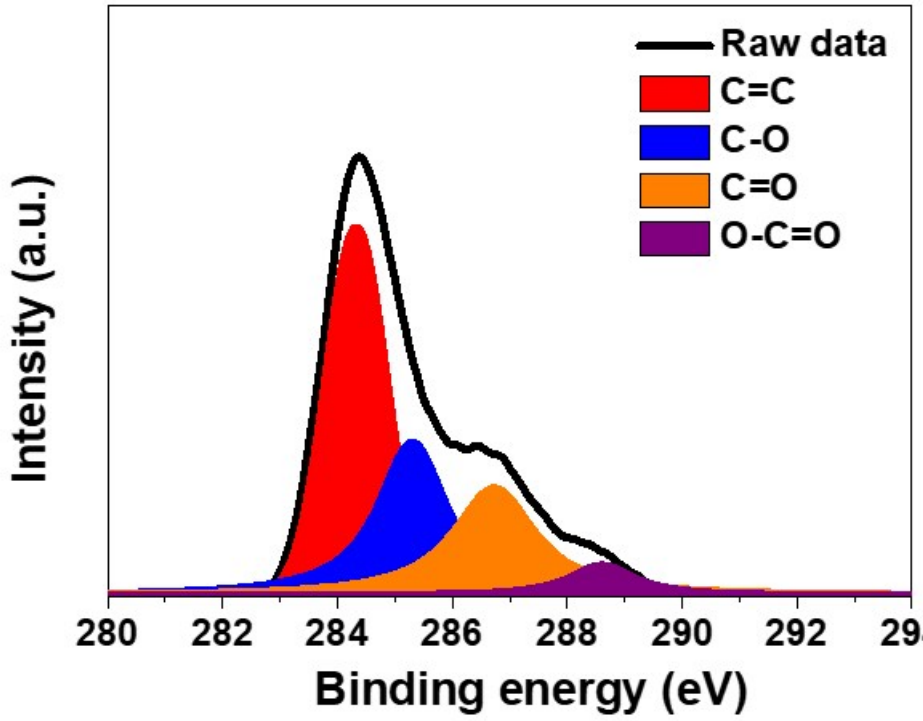

Composition (%)							Sheet Resistance (Ω/sq)
C	O	C/O	C-C /C=C	C-O	C=O	O-C=O	
77.34	22.66	3.42	40.70	29.2	24.5	5.5	8364.6

Figure S6. The XPS C1s core level spectrum on the as-prepared ECG and the conclude C/O ratio, oxygen bonding states. The sheet resistance of ECG film was measured on a glass substrate.

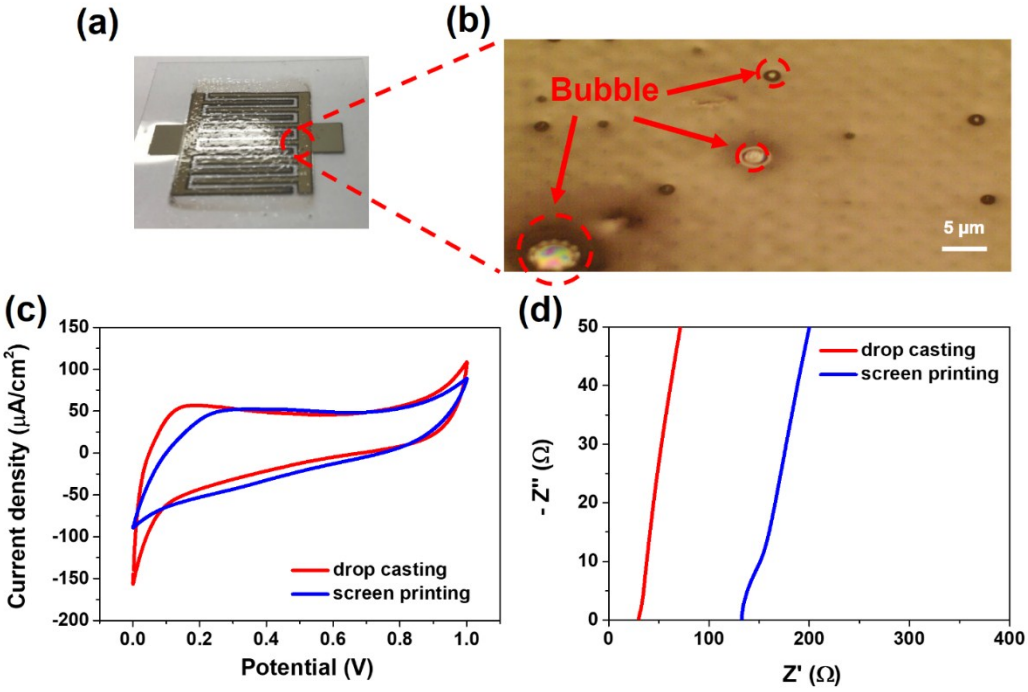

Figure S7. (a) The photo and (b) the OM image of MSCs device after coating electrolyte via screen printing methods. The (c) CV curves (d) EIS profiles of the MSCs device with screen-printed/drop-casted electrolyte.

S8: The CV, GCD, EIS curves of MSC devices with optimized conditions

A series of electrochemical measurements were performed to evaluate our device by two-electrode configuration. Figure S4a,b,d presented the CV, GCD and EIS curves of all screen-printable MSC, respectively. In Figure. 5a, the curves have a large closed area and near rectangular shape at a scan rate of 5 to 200 mV s^{-1}, indicating the characteristics of electrochemical double-layer capacitive behavior. Also, the GCD curves (Fig. S8b) showed nearly triangular shape at different current densities varying from 0.05 to 0.8 mA/cm^2 and without any visible IR drop. The areal capacitance, calculated from the GCD curves (Fig. S8b), with rate capability was shown in Fig. S8c. Electrochemical impedance spectroscopy (EIS) confirmed the fast ion transport of ECG/CNT electrode which exhibiting a straight line closed the Z' axis at low frequency and a small equivalent series resistance (ESR) of 29.7 Ω in the high-frequency region (Fig. S8d). Note that the non-symmetric GCD curves and the relative lower coulombic efficiency was due to the existence of the internal resistance of ECG/CNTs electrode(EIS curves shown in figure 8(c)) and the participation of reaction with oxygen functional groups on ECG. The relatively high charge resistance and functional groups was evidenced by the lower C/O ratio of as-prepared ECG, which seldom reduce its

electrical conductivity(Figure S6).

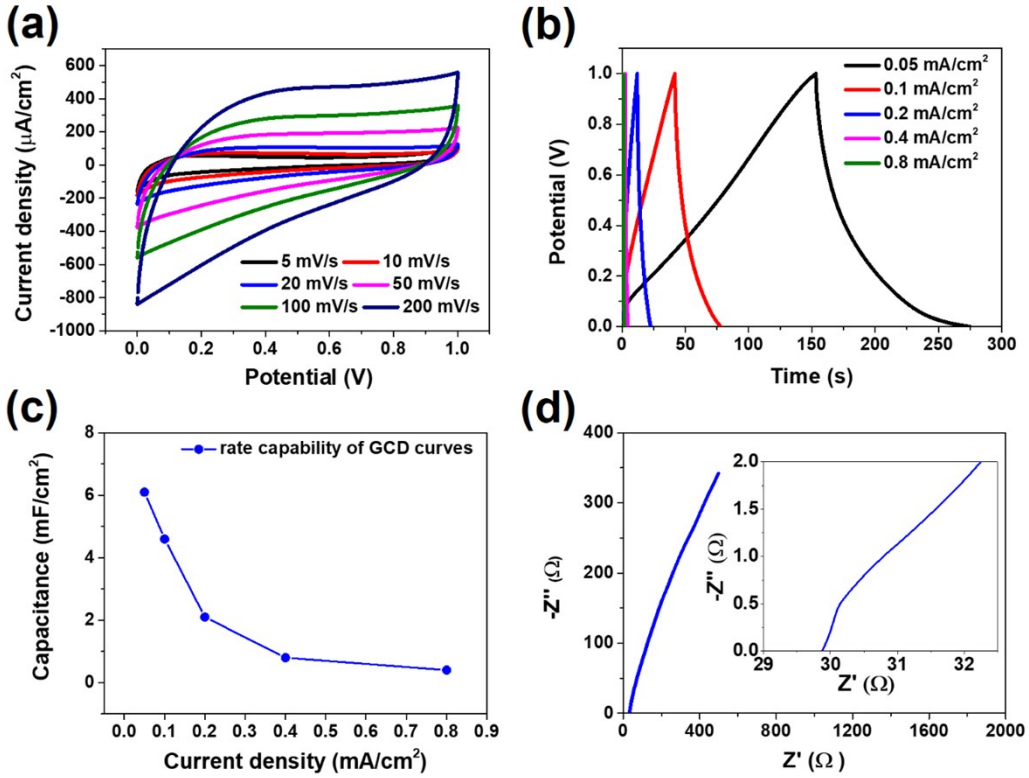

Figure S8. (a) CV curves, (b) GCD, (c) the rate capacitance from GCD curves, and (d) EIS profiles of the MSC with optimized conditions.

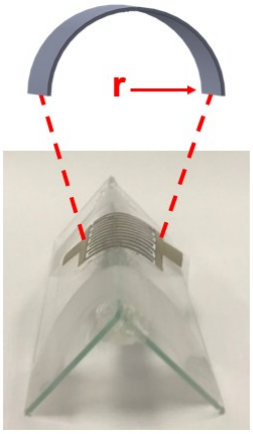

Figure S9. The experimental setup for the bending test of an MSC device, where the radius(r) was defined and estimated.

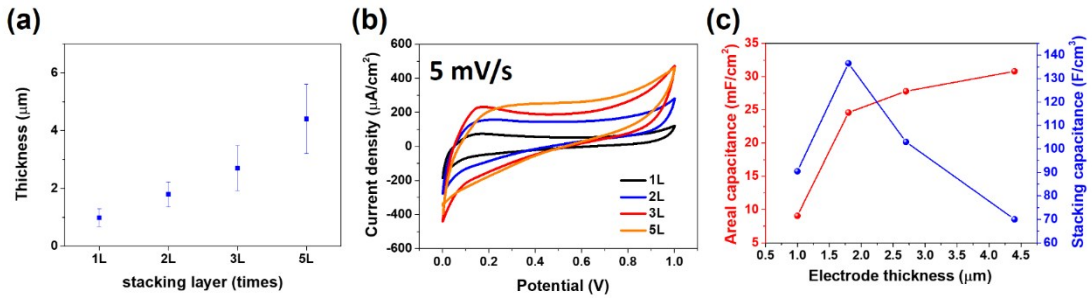

Figure S10 (a) The correlation between the numbers of the stacking layer and thickness. (b) The corresponding CV curve and (c) the areal capacitance.

Table S3. The performance of the MSCs based on different materials and techniques.

material	thickness (µm)	Electrolyte	voltage window	specific areal capacitance (mF/cm^2)	specific stack capacitance (F/cm^3)	Energy density (mWh/cm^3)	Power density (W/cm^3)	Patterning technique
ECG/CNTs	1.00±0.3	PVA-H_3PO_4 (5M)	0-1.0	4.7 (5 $mV*s^{-1}$)	47.0	6.5	0.62	Screen printing (This work)
ECG/CNTs with Ag current collector	1.00±0.3	PVA-H_3PO_4 (2 M)	0-1.0	7.7 (5 $mV*s^{-1}$)	77.3	10.7	3.17	
rGO-PEDOT/PSS [1]	57.90	PVA-H_3PO_4 (1.5M)	0-1.0	84.7 (5 $mV*s^{-1}$)	14.6	2.26	1.21*	Laser etching
EEG [2]	0.75	PSSH-H_3PO_4	0-1.0	0.7 (10 $mV*s^{-1}$)	9.3*	~1.5	~1	Ink-jet printing

MPG[3]	0.015	PVA-H_2SO_4	0-1.0	0.081 (10 $mV*s^{-1}$)	17.9	2.50	495.00	Oxygen plasma etching via mask
graphene-CNT[4]	0.1	Na_2SO_4 (1M)	0-1.0	2.2 (0.2 $V*s^{-1}$)	1.1	0.16	115.00	Photolithograph and CVD
rGO-CNT[5]	0.1	KCl (3M)	0-1.0	6.1 (10 $mV*s^{-1}$)	37.5	0.68	~77	Photolithograph and electrostatic spray
PANI-G[6]	5	PVA-H_2SO_4	0-1.0	196 (10 mV/s-1)	377	10.1	~1.1	Oxygen plasma etching via ma
EG/V_2O_5[7]	0.3	PVA-LiCl	0.-1.0	3.9 (10 $mV*s^{-1}$)	130.7	20	235	Oxygen plasma etching

LSG[8]	7.6	PVA-H_2SO_4	0.-1.0	2.3 (16.8 mA*cm^{-3})	3.0	~0.6	~200	Laser writing
BNG[9]	0.008	PVA-H_2SO_4	0.-1.0	0.3904 (10 mV*s^{-1})*	488	~3.4	~910	Oxygen plasma etching
MnO_2/OLC[10]	10	PVA-H_2SO_4	0-0.8	7.0 (5 mV*s^{-1})	7.0	0.98*	0.85*	Screen printing
PANi[11]	0.4	PVA-H_2SO_4	0-1.0	23.5 (0.1 mA*cm^{-2})*	588	82	1250	Photolithography
rGO/TiO_2[12]	0.063	$EMImNTF_2$	0-3.0	0.5 (50mV*s^{-1})	84.7	7.7	312	UV reduction

N-doping CVD graphene/ PVA-H_3PO_4[13]	20	PVA-H_3PO_4	0-1.0	37.5 (5 $mV*s^{-1}$)	18.75*	2.08	1.6*	gravure printing
$Mg(OH)_2$/GO [14]	10	PVA-H_2SO_4	0-0.8	6.65 (0.1 $mA*cm^{-2}$)	6.65*	1.41	0.3	gravure printing

ECG/CNTs: electrochemical exfoliated graphene/carbon nanotube,

EEG: electrochemically exfoliated graphene, B-LIG: boron-doped laser-induced graphene, MnO_2/OLC: MnO2/onion like carbon, MPG: methane-plasma reduced graphene, EG/V_2O_5: exfoliated graphene/V_2O_5, LSG: laser-scribed graphene, BNG: nitrogen and boron co-doped graphene, PANI-G: polyaniline-functionalized graphene, PANi: polyaniline

*Calculated based on the dimensions given in reference if the specific result were not given in the literature.

Reference

1. Y. Liu, B. Weng, Q. Xu, Y. Hou, C. Zhao, S. Beirne, K. Shu, R. Jalili, G. G. Wallace, J. M. Razal and J. Chen, *Advanced Materials Technologies*, 2016, **1**, 1600166.
2. J. Li, S. Sollami Delekta, P. Zhang, S. Yang, M. R. Lohe, X. Zhuang, X. Feng and M. Ostling, *ACS Nano*, 2017, **11**, 8249-8256.
3. Z. S. Wu, K. Parvez, X. L. Feng and K. Mullen, *Nat. Commun.*, 2013, **4**, 2487.
4. J. Lin, C. Zhang, Z. Yan, Y. Zhu, Z. Peng, R. H. Hauge, D. Natelson and J. M. Tour, *Nano Letters*, 2013, **13**, 72-78.
5. M. Beidaghi and C. Wang, *Advanced Functional Materials*, 2012, **22**, 4501-4510.
6. Z. S. Wu, K. Parvez, S. Li, S. Yang, Z. Y. Liu, S. H. Liu, X. L. Feng and K. Muellen, *Advanced Materials*, 2015, **27**, 4054-4061.
7. P. Zhang, F. Zhu, F. Wang, J. Wang, R. Dong, X. Zhuang, O. G. Schmidt and X. Feng, *Adv Mater*, 2017, **29**.
8. M. F. El-Kady and R. B. Kaner, *Nat. Commun.*, 2013, **4**, 1475.
9. Z.-S. Wu, K. Parvez, A. Winter, H. Vieker, X. Liu, S. Han, A. Turchanin, X. Feng and K. Müllen, *Advanced Materials*, 2014, **26**, 4552-4558.
10. Y. Wang, Y. Shi, C. X. Zhao, J. I. Wong, X. W. Sun and H. Y. Yang, *Nanotechnology*, 2014, **25**, 094010.
11. K. Wang, W. Zou, B. Quan, A. Yu, H. Wu, P. Jiang and Z. Wei, *Advanced Energy Materials*, 2011, **1**, 1068-1072.
12. S. Wang, Z.-S. Wu, S. Zheng, F. Zhou, C. Sun, H.-M. Cheng and X. Bao, *ACS Nano*, 2017, **11**, 4283-4291.
13. Q. Chang, L. Li, L. Sai, W. Shi and L. Huang, *Advanced electronic Materials*, 2018, **4**, 1800059.
14. Z. Qi, H. Lei, C. Quanhong, S. Wangzhou, S. Leo and C. Qi, *Nanotechnology*, 2016, **27**, 105401.